Manipulating and protecting entanglement by means of spin environments

Manipulating and protecting entanglement by means of spin environments

T J G Apollaro[1], **A Cuccoli**[1,2], **C Di Franco**[3], **M Paternostro**[4,8],
F Plastina[5,6] **and P Verrucchi**[1,7]

[1] Dipartimento di Fisica, Università di Firenze, Via G Sansone 1,
I-50019 Sesto Fiorentino (FI), Italy
[2] INFN Sezione di Firenze, via G Sansone 1, I-50019 Sesto Fiorentino (FI), Italy
[3] Department of Physics, University College Cork, Republic of Ireland
[4] School of Mathematics and Physics, Queen's University, Belfast BT7 1NN,
UK
[5] Dipartimento di Fisica, Universitàdella Calabria, 87036 Arcavacata di Rende
(CS), Italy
[6] INFN—Gruppo collegato di Cosenza, 87036 Arcavacata di Rende (CS), Italy
[7] ISC—Consiglio Nazionale delle Ricerche, UO Dipartimento di Fisica,
via G Sansone 1, I-50019 Sesto Fiorentino (FI), Italy
E-mail: m.paternostro@qub.ac.uk

Abstract. We study the dynamical behavior of two initially entangled qubits, each locally coupled to an environment embodied by an interacting spin chain. We consider energy-exchange qubit–environment couplings resulting in rich and highly non-trivial entanglement dynamics. We obtain exact results for the time evolution of the concurrence between the two qubits and find that, by tuning the interaction parameters, one can freeze the dynamics of entanglement, therefore inhibiting their relaxation into the spin environments, as well as activate a sudden-death phenomenon. We also discuss the effects of an environmental quantum phase transition on the features of the two-qubit entanglement dynamics.

[8] Author to whom any correspondence should be addressed.

Contents

1. Introduction

The interplay between coherent and incoherent processes is key to the quantum mechanical processing of information. Systems designed to perform a given communication or computational task have to cope with the detrimental effects of the surrounding world, which can affect an otherwise coherent process in many distinct ways [1]. In the context of distributed quantum information processing (QIP), where networks of spatially remote quantum nodes are used in order to process information in a delocalized way, a good assumption is that each local processor is affected by its own environment. Such an architecture for a QIP device is currently at the focus of extensive and multifaceted theoretical and experimental endeavors [2].

Extensive work has been performed on the incoherent dynamics resulting from the coupling of QIP systems with baths weakly perturbed by the system-induced back-action. The loss of quantum correlations due to the environment has recently received considerable attention [3], with particular emphasis on the phenomenon of environment-induced entanglement sudden death (ESD) [4] (i.e. complete disentanglement in a finite time), which has also been experimentally tested for the case of electromagnetic environments [5]. And yet, especially for solid-state implementations of quantum processors, the case of structured environments is extremely relevant [6]. In this framework, the dynamics leading to complete disentanglement of two qubits coupled with common spin environments (the so-called 'central-qubit model') have been extensively studied [7]–[9]. Exponential decay of the concurrence [10] between two qubits initially prepared in pure states has been observed, the decay rate being enhanced for working points close to the quantum phase transition (QPT) of the environment [8].

In this paper, we study the dynamical evolution of the entanglement between two remote qubits coupled with mutually independent spin environments. The exact time dependence of their reduced density matrix is obtained using an original approach [12]–[14] that allows us to track the dynamics of quantum averages of one- and two-spin observables and entanglement properties. In stark contrast with most of the available literature, here we consider a 'transversal' qubit–environment coupling that allows for energy transfer, resulting in a dissipative-like behavior of the qubits and in a much richer entanglement dynamics.

The transversal nature of the qubit–environment coupling allows us to reveal the occurrence of entanglement sudden death, even when starting from initially pure states of the qubits, which included the maximally entangled ones that are extremely relevant for QIP. The above feature cannot emerge in the case of longitudinal couplings, as reported in [7]–[9], [11].

IOP Institute of Physics **Φ**DEUTSCHE PHYSIKALISCHE GESELLSCHAFT

We show that, by setting the environment in different operating regimes, one can induce either entanglement sudden death or a freezing effect. Moreover, we shed light on the differences in behavior experienced by the *parallel* and *antiparallel* concurrences introduced in [16], whose interplay is crucial in determining the properties of the quantum correlations within the two-qubit state, in particular at the environmental quantum critical point where the antiparallel entanglement appears to be better preserved than the parallel one.

This paper is organized as follows. In section 2, we define the physical system and the relevant interactions. In section 3, we provide exact expressions for the dynamics of a single qubit coupled with a spin–environment. These results are used in section 4 to obtain the dynamics of the entanglement between two qubits, each coupled with a spin–environment via a local isotropic (section 4.1) or anisotropic (section 4.2) exchange interaction. Finally, in section 5, we draw some conclusions and suggest a possible scenario where the main features of our physical model can be embodied.

2. The system

We consider two non-interacting subsystems, A and B, each consisting of a qubit Q_κ ($\kappa = A, B$) coupled with a chain Γ_κ of N_κ interacting $S = 1/2$ particles. Whenever useful, we will hereafter use the index $\kappa = A, B$ so as to generically refer to either of the two subsystems, A or B. As usual, the qubits Q_κ are described in terms of $S = 1/2$ spin operators, which we indicate as $\hat{s}_{0\kappa}$. Operator $\hat{s}_{n_\kappa}$ ($n_\kappa = 1, \ldots, N_\kappa$) corresponds to the spin located at site n of the chain Γ_κ. Note that although the above notation suggests the spin describing Q_κ to sit at site 0 of the respective chain Γ_κ, this is just a useful convention; it has no implication about the physical nature of Q_A and Q_B.

The intra-chain interaction is of XY-Heisenberg-type with local magnetic fields possibly applied in the z-direction,

$$\hat{\mathcal{H}}_{\Gamma_\kappa} = -2 \sum_{n_\kappa=1}^{N_\kappa-1} (J_{n_\kappa}^x \hat{s}_{n_\kappa}^x \hat{s}_{n_\kappa+1}^x + J_{n_\kappa}^y \hat{s}_{n_\kappa}^y \hat{s}_{n_\kappa+1}^y) - 2 \sum_{n_\kappa=1}^{N_\kappa} h_{n_\kappa} \hat{s}_{n_\kappa}^z, \tag{1}$$

where h_{n_κ} is the field applied at site n_κ and $J_{n_\kappa}^{x,y}$ are the coupling strengths of the intra-chain interactions. Each Γ_κ is open-ended, while neither the $J_{n_\kappa}^{x,y}$'s nor the magnetic fields h_{n_κ} need to be uniform along the chains. Qubit Q_κ is coupled with the first spin of its environment, embodied by Γ_κ, via an exchange interaction of strengths $J_{0_\kappa}^{x,y}$ and can be subjected to a local magnetic field h_{0_κ} directed along the z-direction. The corresponding Hamiltonian reads

$$\hat{\mathcal{H}}_{0_\kappa} = -2(J_{0_\kappa}^x \hat{s}_{0_\kappa}^x \hat{s}_{1_\kappa}^x + J_{0_\kappa}^y \hat{s}_{0_\kappa}^y \hat{s}_{1_\kappa}^y) - 2h_{0_\kappa} \hat{s}_{0_\kappa}^z. \tag{2}$$

The Hamiltonian of the total system κ is thus given by $\hat{\mathcal{H}}_\kappa = \hat{\mathcal{H}}_{0_\kappa} + \hat{\mathcal{H}}_{\Gamma_\kappa}$. In figure 1, we provide a sketch of the model considered. As stated previously, although A and B do not interact directly, they experience joint dynamics due to the possibility of sharing initial entanglement. Depending on the choice of the local interaction parameters and magnetic fields in $\hat{\mathcal{H}}_\kappa$, the effort required to tackle the model greatly changes. In section 3, we describe the approach used to achieve an exact solution for the dynamics of local observables.
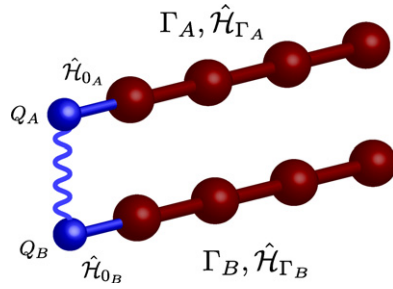
Figure 1. Sketch of the physical model. Each of a pair of entangled qubits, Q_A and Q_B, is locally coupled with a spin chain, Γ_A and Γ_B, via the Hamiltonians $\hat{\mathcal{H}}_{0_A}$ and $\hat{\mathcal{H}}_{0_B}$, respectively. The dynamics within each chain are ruled by the intra-chain Hamiltonians, $\hat{\mathcal{H}}_{\Gamma_A}$ and $\hat{\mathcal{H}}_{\Gamma_B}$. The wavy line indicates the initial entanglement.

3. Exact single-qubit dynamics

We first concentrate on the dynamics of one subsystem only (thus dropping the index κ throughout this section). In particular, we are interested in the evolution of a given initial state of the qubit Q, as determined by its coupling with the chain Γ and under the influence of the local magnetic field. We resort to the Heisenberg picture, which has recently been shown to provide a convenient framework for the analysis of quantum many-body systems of interacting particles [12]. The key step is the use of the Campbell–Baker–Hausdorff (CBH) formula in the management of the time-evolution operator of the system. For an operator $\hat{\mathcal{O}}$ associated with an observable of a physical system with Hamiltonian $\hat{\mathcal{H}}$, the CBH formula reads (we set $\hbar = 1$ throughout the paper)

$$\hat{\mathcal{O}}(t) = \sum_{p=0}^{\infty} \frac{(\mathrm{i}t)^p}{p!} \left[\hat{\mathcal{H}}, \left[\hat{\mathcal{H}}, \cdots \left[\hat{\mathcal{H}}, \hat{\mathcal{O}} \right] \cdots \right] \right]. \tag{3}$$

By virtue of the algebra satisfied by the Pauli matrices, we find that, upon application of equation (3), the time evolution of the components of $\hat{s}_0$ reads

$$\hat{s}_0^x(t) = \frac{1}{2} \sum_{n=0}^{N} \left[\Pi_n^x(t)\hat{\sigma}_n^x + \Delta_n^x(t)\hat{\sigma}_n^y \right] \hat{P}_n,$$

$$\hat{s}_0^y(t) = \frac{1}{2} \sum_{n=0}^{N} \left[\Pi_n^y(t)\hat{\sigma}_n^y - \Delta_n^y(t)\hat{\sigma}_n^x \right] \hat{P}_n, \tag{4}$$

$$\hat{s}_0^z(t) = -\mathrm{i}2\hat{s}_0^x(t)\hat{s}_0^y(t),$$

where $\hat{\sigma}_n^\alpha$ ($\alpha = x, y, z$) are the Pauli operators for the spin at site n and $\hat{P}_n = \prod_{i=0}^{n-1} \hat{\sigma}_i^z$. The time-dependent coefficients $\Pi_n^x(t)$ and $\Delta_n^x(t)$ are the components of the $(N+1)$-dimensional vectors

$\mathbf{\Pi}^x(t)$ and $\mathbf{\Delta}^x(t)$ defined by

$$\mathbf{\Pi}^x(t) = \sum_{p=0}^{\infty} (-1)^p \frac{t^{2p}}{(2p)!} (\boldsymbol{\tau}\boldsymbol{\tau}^{\mathrm{T}})^p \boldsymbol{v}, \tag{5}$$

$$\mathbf{\Delta}^x(t) = \sum_{p=0}^{\infty} (-1)^p \frac{t^{2p+1}}{(2p+1)!} \boldsymbol{\tau}^{\mathbf{T}} (\boldsymbol{\tau}\boldsymbol{\tau}^{\mathrm{T}})^p \boldsymbol{v}, \tag{6}$$

where 'T' stands for transposition, the vector $\boldsymbol{v}$ has components $v_i = \delta_{i0}$ [15] and the tri-diagonal matrix $\boldsymbol{\tau}$ has elements

$$\tau_{ij} = J_{i-1}^y \delta_{i-1,j} + J_i^y \delta_{i+1,j} - 2h_i \delta_{i,j}. \tag{7}$$

The coefficients $\mathbf{\Pi}^y(t)$ and $\mathbf{\Delta}^y(t)$ are obtained from equations (5) and (6) by replacing $\boldsymbol{\tau}$ with $\boldsymbol{\tau}^{\mathrm{T}}$. As $\boldsymbol{\tau}\boldsymbol{\tau}^{\mathrm{T}}$ is real and symmetric, there is an orthogonal matrix $\boldsymbol{U}$ that diagonalizes it, so that $(\boldsymbol{\tau}\boldsymbol{\tau}^{\mathrm{T}})^p = \boldsymbol{U}\boldsymbol{\Lambda}^{2p}\boldsymbol{U}^{\mathrm{T}}$, with $\boldsymbol{\Lambda}$ being the diagonal matrix whose elements $\lambda_{ij} = \lambda_i \delta_{i,j}$ are the (positive) square roots of the eigenvalues of $\boldsymbol{\tau}\boldsymbol{\tau}^{\mathrm{T}}$. Similarly, there is an orthogonal matrix $\boldsymbol{V}$ that diagonalizes $\boldsymbol{\tau}^{\mathrm{T}}\boldsymbol{\tau}$ such that $(\boldsymbol{\tau}^{\mathrm{T}}\boldsymbol{\tau})^p = \boldsymbol{V}\boldsymbol{\Lambda}^{2p}\boldsymbol{V}^{\mathrm{T}}$ with the same diagonal matrix $\boldsymbol{\Lambda}$ as above. As a consequence, after straightforward matrix algebra, one can sum up the time-dependent series in equations (5) and (6) to obtain

$$\mathbf{\Pi}^x(t) = \boldsymbol{U}\boldsymbol{\Omega}(t)\boldsymbol{U}^{\mathrm{T}}\boldsymbol{v}, \quad \mathbf{\Delta}^x(t) = \boldsymbol{V}\boldsymbol{\Sigma}(t)\boldsymbol{U}^{\mathrm{T}}\boldsymbol{v},$$

$$\mathbf{\Pi}^y(t) = \boldsymbol{V}\boldsymbol{\Omega}(t)\boldsymbol{V}^{\mathrm{T}}\boldsymbol{v}, \quad \mathbf{\Delta}^y(t) = \boldsymbol{U}\boldsymbol{\Sigma}(t)\boldsymbol{V}^{\mathrm{T}}\boldsymbol{v}, \tag{8}$$

where $\boldsymbol{\Omega}(t)$ and $\boldsymbol{\Sigma}(t)$ are diagonal matrices with elements $\Omega_{ij}(t) = \cos(\lambda_i t)\delta_{ij}$ and $\Sigma_{ij}(t) = \sin(\lambda_i t)\delta_{ij}$. The above equations hold regardless of the local magnetic fields or the couplings $J_n^{x,y}$ and $J_0^{x,y}$. Adopting the language of [12]–[14], the components of $\mathbf{\Pi}^{x,y}(t)$ and $\mathbf{\Delta}^{x,y}(t)$ embody the *fluxes of information* from the qubit Q to the spin chain Γ.

By means of equations (4), one can determine the time evolution of the single-qubit density matrix,

$$\hat{\rho}_0(t) = \frac{1}{2}\hat{\mathbb{1}} + \sum_{\alpha} \langle \hat{s}_0^\alpha(t) \rangle \hat{\sigma}_0^\alpha, \tag{9}$$

where $\hat{\mathbb{1}}$ is the identity operator and $\langle \cdot \rangle$ indicates the expectation value over the initial state of the system. Once the diagonalizations required for determining the vectors $\mathbf{\Pi}^{x(y)}(t)$ and $\mathbf{\Delta}^{x(y)}(t)$ are performed, we need to evaluate the expectation values entering equation (9). Such a task can be performed within two different scenarios. In the first, Γ has a small number of spins, so that one can design the precise structure of its initial state. In the second, Γ consists of a large number of spins, which puts the analysis in the thermodynamic limit, where we can benefit from specific symmetry properties of $\hat{\mathcal{H}}_\Gamma$. Here, we concentrate on the latter situation, which has been the subject of several recent papers, due to the fact that it can be used for describing a proper qubit–environment system.

We assume that Q and Γ are initially uncorrelated and set the former in an arbitrary single-qubit state $\hat{\rho}_0$ and the latter in an eigenstate $|\Psi_\Gamma\rangle$ of $\hat{\mathcal{H}}_\Gamma$. The initial state of the total system will thus be $\hat{\rho} = \hat{\rho}_0 \otimes |\Psi_\Gamma\rangle \langle \Psi_\Gamma|$. Under such conditions, the procedure described in the above section is most conveniently implemented, as equations (4) greatly simplify due to the properties

of $\hat{\mathcal{H}}_\Gamma$. In particular, the conservation rule $[\hat{\mathcal{H}}, \bigotimes_{n=0}^N \hat{\sigma}_n^z] = 0$, which states parity invariance of the Hamiltonian, together with the property $\langle \hat{\sigma}_n^\alpha \hat{\sigma}_m^\beta \rangle = 0$ for $\alpha \neq \beta$ and $n \neq m$, implies[9]

$$\langle \hat{s}_0^x(t) \rangle = \frac{1}{2} \sum_{n=0}^N \left[\Pi_n^x(t) \langle \hat{P}_n \hat{\sigma}_n^x \rangle + \Delta_n^x(t) \langle \hat{P}_n \sigma_n^y \rangle \right], \tag{10}$$

$$\langle \hat{s}_0^y(t) \rangle = \frac{1}{2} \sum_{n=0}^N \left[\Pi_n^y(t) \langle \hat{P}_n \hat{\sigma}_n^y \rangle - \Delta_n^y(t) \langle \hat{P}_n \hat{\sigma}_n^x \rangle \right], \tag{11}$$

$$\begin{aligned}
\langle \hat{s}_0^z(t) \rangle = {} & \frac{1}{2} \sum_{n=0}^N \left[\Pi_n^x(t) \Pi_n^y(t) + \Delta_n^x(t) \Delta_n^y(t) \right] \langle \hat{\sigma}_n^z \rangle \\
& - \frac{1}{2} \sum_{n<m}^N \left[\Pi_n^y(t) \Pi_m^x(t) + \Delta_n^x(t) \Delta_m^y(t) \right] \langle \hat{P}_{n+1} \hat{P}_m \hat{\sigma}_n^x \hat{\sigma}_m^x \rangle \\
& - \frac{1}{2} \sum_{n<m}^N \left[\Pi_n^x(t) \Pi_m^y(t) + \Delta_n^y(t) \Delta_m^x(t) \right] \langle \hat{P}_{n+1} \hat{P}_m \hat{\sigma}_n^y \hat{\sigma}_m^y \rangle.
\end{aligned} \tag{12}$$

Using equations (9)–(12), one can finally evaluate the single-qubit density matrix $\hat{\rho}_0(t)$.

4. Exact two-qubit dynamics

We now consider the complete system $A \cup B$. Under the assumption of non-interacting subsystems, the time propagator generated by $\hat{\mathcal{H}}_A + \hat{\mathcal{H}}_B$ factorizes as $\hat{\mathcal{U}}_A(t) \otimes \hat{\mathcal{U}}_B(t)$ with $\hat{\mathcal{U}}_\kappa(t) = \exp[-i\hat{\mathcal{H}}_\kappa t]$. Despite the absence of interaction, A and B might still display dynamical correlations depending on the initial state of the total system. In fact, if $A \cup B$ is prepared in an entangled state, its dynamical properties will depend on the structure of such an initial state and the entanglement evolution will follow from the interactions ruling A and B separately. The values of the parameters entering $\hat{\mathcal{H}}_\kappa$ might thus be considered as *knobs* for the entanglement dynamics.

We prepare the total system at time $t = 0$ in

$$\hat{\rho}(0) = \hat{\rho}^{Q_A Q_B}(0) \otimes \hat{\rho}^{\Gamma_A}(0) \otimes \hat{\rho}^{\Gamma_B}(0), \tag{13}$$

so that we can use the results of section 3 and write the two-qubit density matrix at time t in terms of the time-evolved single-qubit one. In fact, using the results of Bellomo *et al* [15], we have

$$\rho_{ij}^{Q_\kappa}(t) = \sum_{p,r} K_{ij}^{pr}(t) \rho_{pr}^{Q_\kappa}(0), \quad (\kappa, K = A, B), \tag{14}$$

with $\rho_{ij}^{Q_\kappa}(t)$ being the elements of the single-qubit density matrix at time t and $\boldsymbol{K}$ a tensor of time-dependent coefficients. The two-qubit state can then be written as

$$\rho_{IJ}^{Q_A Q_B}(t) = \sum_{p_A, r_A} \sum_{p_B, r_B} A_{i_A j_A}^{p_A r_A}(t) B_{i_B j_B}^{p_B r_B}(t) \rho_{PR}^{Q_A Q_B}(0), \tag{15}$$

---

[9] In order to establish a clear relation with the site-ordering in the physical model at hand, we label columns and rows of $(N+1) \times (N+1)$ matrices and $(N+1)$-dimensional vectors involved in our formalism using indices ranging from 0 to N.

where lower-case indices take values 1 and 2, while capital ones are defined according to $L = l_A + l_B - l_A \bmod 2 = 1, \ldots, 4$ (with $L = I, J, P, R$ and $l = i, j, p, r$). By setting $\hat{\rho}_{\Gamma_\kappa}(0) = \left| \Psi_{\Gamma_\kappa} \right\rangle \left\langle \Psi_{\Gamma_\kappa} \right|$, i.e. by preparing both the chains in any of the eigenstates of their respective Hamiltonians, we can explicitly evaluate equations (10)–(12) and hence equation (9). By comparing the latter with equation (14), we finally determine the coefficients $K_{ij}^{pr}(t)$, thus fully specifying the dynamics of the two-qubit state $\hat{\rho}^{Q_A Q_B}(t)$.

Our approach is fully general and can be used in a variety of different situations. Here we concentrate on the case where the initial state of the two qubits is one of the Bell states,

$$|\phi_\pm\rangle = \frac{1}{\sqrt{2}} \left(|00\rangle \pm |11\rangle \right), \quad |\psi_\pm\rangle = \frac{1}{\sqrt{2}} \left(|01\rangle \pm |10\rangle \right), \tag{16}$$

which we dub *parallel* ($|\phi_\pm\rangle$) and *antiparallel* ($|\psi_\pm\rangle$) Bell states [16]. By virtue of the symmetries of such states, the concurrence of the two-qubit state can be written as $C(t) = 2 \max\{0, C_{\uparrow\uparrow}(t), C_{\uparrow\downarrow}(t)\}$, where we have introduced

$$C_{\uparrow\downarrow}(t) = |\tilde{\rho}_{23}| - \sqrt{\tilde{\rho}_{11}\tilde{\rho}_{44}}, \tag{17}$$

$$C_{\uparrow\uparrow}(t) = |\tilde{\rho}_{14}| - \sqrt{\tilde{\rho}_{22}\tilde{\rho}_{33}}, \tag{18}$$

with $C_{\uparrow\uparrow}(0) = 1$ for $\hat{\rho}_0^{Q_A Q_B}(0) = |\phi_\pm\rangle \langle \phi_\pm|$ and $C_{\uparrow\downarrow}(0) = 1$ for $\hat{\rho}_0^{Q_A Q_B}(0) = |\psi_\pm\rangle \langle \psi_\pm|$. Here the notation $\tilde{\rho}_{IJ}$ is used, for the sake of clarity, to indicate the matrix elements $\rho_{IJ}^{Q_A Q_B}(t)$ defined in equation (15). In what follows, $C_a(t)$ [$C_p(t)$] is the concurrence corresponding to the case where the qubits are initially prepared in an antiparallel [parallel] Bell state.

As for the environments, we take two identical chains of an (equal) even number of spins N with homogeneous intra-chain couplings and field, i.e. $J_{n_\kappa}^{x,y} = J$ and $h_{n_\kappa} = h$. Both chains are prepared in the ground state of $\mathcal{H}_{\Gamma_\kappa}$, which is found via Jordan–Wigner and Fourier transformations [17, 18]. Straightforward calculations yield the relevant mean values entering equations (4) as

$$\langle \hat{\sigma}_n^z \rangle = 1 - \frac{2}{N+1} \left(k_F - \frac{\cos[(k_F + 1)\vartheta_n] \sin[k_F \vartheta_n]}{\sin \vartheta_n} \right),$$

$$g_{nm} \equiv \langle \hat{P}_n \hat{P}_m \hat{\sigma}_n^x \hat{\sigma}_m^x \rangle = \frac{\varphi_{n,k_F+1} \varphi_{m,k_F} - \varphi_{n,k_F} \varphi_{m,k_F+1}}{2(\cos \vartheta_n - \cos \vartheta_m)}, \tag{19}$$

where, for convenience of notation, we omit the index κ. We have introduced $\varphi_{j,k} = \sqrt{2/(N+1)} \sin(j\vartheta_k)$, $\vartheta_k = k\pi/(N+1)$, $k \in [1, N]$ and the Fermi wave number k_F is determined by the magnetic field [18]. Moreover, due to the absence of symmetry breaking in $|\Psi_{\Gamma_\kappa}\rangle$, it is $\langle \hat{\sigma}_{n_\kappa}^{x,y} \rangle = 0$. We consider N finite but large enough to avoid finite-size effects to influence our results. For the range of parameters considered here, $N = 50$ is found to fulfil such a condition and it is then chosen to set the length of both chains. Finally, we take the same coupling strength between each qubit and its chain, i.e. $J_{0_\kappa}^\alpha = J_0^\alpha$.

4.1. Isotropic coupling between the qubit and the chain

We now consider an isotropic coupling between each qubit and its respective environment, defined by $J_{0_\kappa}^x = J_{0_\kappa}^y = J_0$ in equation (2). In the theory of open quantum systems, such coupling

typically corresponds to a dissipative interaction treated in the rotating wave approximation [19]. For isotropic coupling, the total Hamiltonians $\hat{\mathcal{H}}_\kappa$ have rotational invariance along the z-axis. This implies that $\boldsymbol{\tau} = \boldsymbol{\tau}^{\mathrm{T}}$ and thus $\Pi_n^x(t) = \Pi_n^y(t) \equiv \Pi_n(t)$, $\Delta_n^x(t) = \Delta_n^y(t) \equiv \Delta_n(t)$, which allows us to write

$$\langle \hat{s}_0^x(t) \rangle = \tfrac{1}{2}(\Pi_0(t)\langle \hat{\sigma}_0^x \rangle + \Delta_0(t)\langle \hat{\sigma}_0^y \rangle),$$

$$\langle \hat{s}_0^y(t) \rangle = \tfrac{1}{2}(\Pi_0(t)\langle \hat{\sigma}_0^y \rangle - \Delta_0(t)\langle \hat{\sigma}_0^x \rangle),$$

$$\langle \hat{s}_0^z(t) \rangle = \frac{1}{2}\sum_{n=0}^{N}[\Pi_n^2(t) + \Delta_n^2(t)]\langle \hat{\sigma}_n^z \rangle - \frac{1}{4}\sum_{n\neq m=1}^{N}[\Pi_n(t)\Pi_m(t) + \Delta_n(t)\Delta_m(t)]g_{nm}. \tag{20}$$

From the above expressions, we see that single-qubit states initially directed along the z-axis of the Bloch sphere maintain such alignment regardless of the Hamiltonian parameters. On the other hand, initial 'equatorial' states with $\langle \hat{s}_0^z(0) \rangle = 0$ evolve in time and remain on the equatorial plane only for zero overall magnetic field. The rotational invariance around the z-axis of the total Hamiltonians $\hat{\mathcal{H}}_A$ and $\hat{\mathcal{H}}_B$ has relevant consequences also on the evolution of the entanglement, as shown in section 4.2.

In the fully homogeneous case, i.e. for $h_0 = h$ and $J_0 = J$, it is $\lambda_q = -2(h - \cos\frac{q\pi}{N+2})$ and the jth component of the corresponding eigenvector has the same form as $\varphi_{j,q}$ with $N+1$ replaced by $N+2$. Hereafter, time will be measured in units of J^{-1}. In the thermodynamic limit where $N \to \infty$, the summations can be replaced by integrals yielding

$$\langle \hat{s}_0^x(t) \rangle = \frac{\mathcal{J}_1(2t)}{2t}\left[\cos(2ht)\langle \hat{\sigma}_0^x \rangle - \sin(2ht)\langle \hat{\sigma}_0^y \rangle\right],$$

$$\langle \hat{s}_0^y(t) \rangle = \frac{\mathcal{J}_1(2t)}{2t}\left[\cos(2ht)\langle \hat{\sigma}_0^y \rangle + \sin(2ht)\langle \hat{\sigma}_0^x \rangle\right], \tag{21}$$

and, for the z component,

$$\langle \hat{s}_0^z(t) \rangle = \sum_{n=0}^{N} \frac{(n+1)^2}{2t^2}\mathcal{J}_{n+1}^2(2t)\langle \hat{\sigma}_n^z \rangle$$

$$- \sum_{n\neq m}^{n,m\,even} (-1)^{(n+m)/2}\frac{(n+1)(m+1)}{4t^2}\mathcal{J}_{n+1}(2t)\mathcal{J}_{m+1}(2t)g_{nm}$$

$$+ \sum_{n\neq m}^{n,m\,odd} (-1)^{(n+m)/2}\frac{(n+1)(m+1)}{4t^2}\mathcal{J}_{n+1}(2t)\mathcal{J}_{m+1}(2t)g_{nm}, \tag{22}$$

where $\mathcal{J}_n(x)$ are the Bessel functions. Long-time expansions show that the mean value of the single-spin $x(y)$ component decays as $t^{-3/2}$. If $h_0 = h = 0$, equation (22) reduces to $\langle s_0^z(t) \rangle = \gamma(t)\langle \hat{\sigma}_0^z \rangle$ with $\gamma(t) = \mathcal{J}_1^2(2t)/2t^2$, yielding a t^{-3} scaling at long times. Equations (21) and (22) give an excellent approximation also for finite N ($\lesssim 50$) within a time range where finite-size
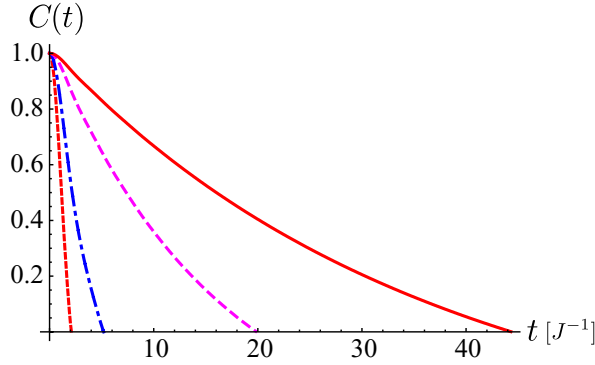
Figure 2. Concurrence between Q_A and Q_B for isotropic and weak coupling, $J_0/J = 0.5, 0.4, 0.2$ and 0.125 (going from the left-most to the right-most curve). No magnetic field is applied.

effects have not yet occurred. As the latter are caused by the reflection of propagating excitations at the boundary of the chain, we can neglect finite-size effects for times up to $\sim N$. In fact, as the maximum one-excitation group velocity is 2, it takes at least a time N for an excitation to leave Q and travel back to it.

Let us now analyze the evolution of the entanglement between the two qubits. We first notice that in the present case of isotropic coupling between Q_κ and Γ_κ, and given that the exchange interaction along the chain is set to be of XX type, both Hamiltonians $\hat{\mathcal{H}}_\kappa$ have rotational invariance around the z-axis. This enforces disjoint dynamics of the off-diagonal matrix elements ($\tilde{\rho}_{23}$ and $\tilde{\rho}_{14}$) entering equation (17) and (18). As a consequence, if $C_{\uparrow\downarrow}(0) = 0$ it is $C_{\uparrow\downarrow}(t) = 0$ at any time (the same holds for $C_{\uparrow\uparrow}(t)$). Moreover, we find that $C_a(t) \geqslant C_p(t)$ for any symmetric $\boldsymbol{\tau}$, irrespective of the Hamiltonian parameters. This means that antiparallel entanglement is more resilient to the effects of the spin environment. Using the analytical solutions given above, we finally obtain the time evolution of the concurrence. For $h = 0$ and in the fully homogeneous case of $J_0 = J$, we find

$$C(t) = 2 \max \left\{ 0, \gamma^2(t) + \gamma(t) - \tfrac{1}{2} \right\}, \tag{23}$$

from which, by using the definition of $\gamma(t)$ in terms of Bessel functions, we infer that at $t_{\text{ESD}} \simeq 0.9037$, ESD occurs. In fact, our results show that sudden death occurs also for $J_0 \neq J$, exhibiting coupling-dependent characteristics. It is remarkable that disentanglement at finite time occurs, here, for pure initial states of the two qubits, a feature due to the specific form of qubit–environment coupling considered here.

In the weak coupling regime $J_0 \ll J$, figure 2 shows that the concurrence relaxation time grows as J_0 decreases. On the other hand, for strong coupling $J_0 \gg J$, the non-Markovian character of the environments becomes evident (as shown in figure 3), and entanglement revivals occur due to the finite memory time of the spin chain. These revivals can be intuitively understood as the result of the strong coupling between the two-qubit system and the spins at the first site of each chain. A large J_0 gives rise to almost perfectly coherent interactions within such a qubit-spin pair, only weakly damped by leakage into the rest of the chains. A revival time (the time after which the revival exhibits a maximum) of about π/J_0 is inferred from figure 3, for $J_0/J \gg 1$. In figure 4(a), such findings are summarized in terms of the dependence
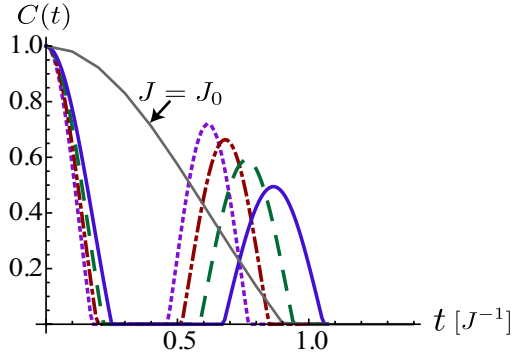
Figure 3. Concurrence between Q_A and Q_B for isotropic and strong couplings, $J_0/J = 3.5, 4, 4.5$ and 5 (solid, dashed, dot-dashed and dotted curves, respectively). No magnetic field is applied. We also show the case of $J_0/J = 1$.
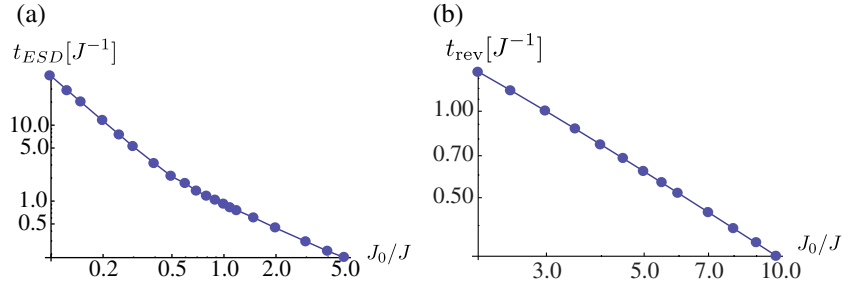

Figure 4. (a) Time t_{ESD} after which the concurrence between Q_A and Q_B first exactly vanishes (entanglement sudden death), as a function of the coupling J_0/J (double logarithmic scale). No magnetic field is applied. (b) Entanglement revival time against $\log_{10}[J_0/J]$. No magnetic field is applied.

of $\log_{10}[t_{\text{ESD}}]$ on $\log_{10}[J_0/J]$. The quasi-linear trend shown there reveals that the growing rate of t_{ESD} for $J_0/J < 1$ is slightly larger than the decreasing rate at $J_0/J > 1$. In figure 4(b), we show the behavior of the revival time against $\log_{10}[J_0/J]$, which also exhibits a quasi-linear trend.

The presence of finite magnetic fields significantly changes the dynamics of the entanglement. If $h_0 > 0$ and $h = 0$, i.e. if the field is only applied to the qubits, then we expect an effective decoupling of each qubit from the dynamics of its environment, such that both $\hat{s}_{0_\kappa}$ precess with a Larmor frequency that depends mostly on h_0, although it is subjected to small quantitative corrections due to the interaction with Γ_κ at rate J_0. In fact, in figure 5, we see that a larger amount of entanglement is maintained for considerably longer times as h_0 grows. Due to the above decoupling, as well as the condition $h_{0_A} = h_{0_B}$, correlations between Q_A and Q_B are preserved and so is their concurrence.

In figure 5(b), the same effect is illustrated by the time-averaged concurrence $\bar{C}_{a,p} = (1/\delta t) \int_{\delta t} C_{a,p}(t')dt'$ (the average is calculated over a time window δt that excludes the oscillatory transients observed in figure 5(a) for $Jt \lesssim 10$ and $Jt \gtrsim 45$). The average entanglement grows with h_0. We further note that parallel and antiparallel concurrences are
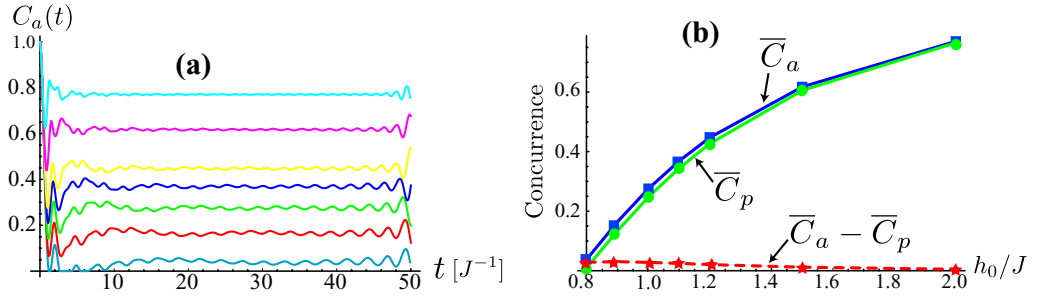
Figure 5. (a) $C_a(t)$ versus t, for isotropic and homogenous couplings ($J_0 = J$) on the chains with $h_\kappa = 0$ and $h_0/J = 0.8, 0.9, 1, 1.1, 1.2, 1.5$ and 2 (from the bottom to the top curve). (b) Average parallel and anti-parallel concurrences and their difference plotted against h_0 with the same parameters as in (a). The lines joining the data points are simply a guide to the eye.
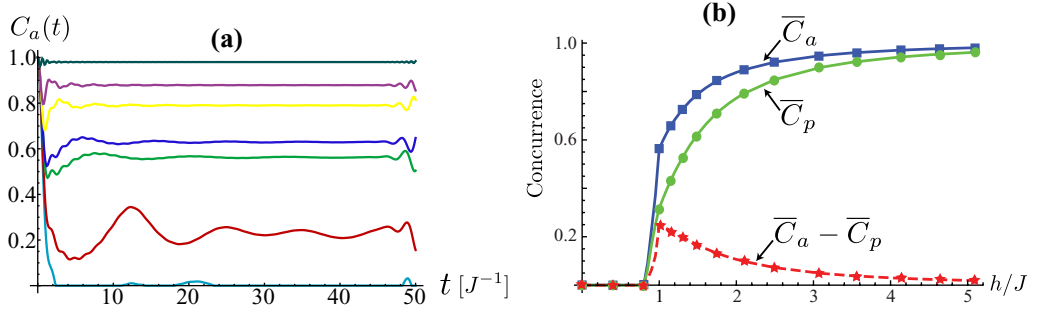

Figure 6. (a) $C_a(t)$ versus t, for isotropic and homogenous couplings ($J_0 = J$), with no field applied on the qubits ($h_{0_\kappa} = 0$) and $h/J = 0.8, 0.9, 1, 1.1, 1.5$ and 2 and 5 (from the bottom to the top curve). (b) Average parallel and anti-parallel concurrences and their difference plotted against h/J with the same parameters as in (a). The lines joining the data points are simply a guide to the eye.

almost identical (with $\bar{C}_a > \bar{C}_p$ as expected), although their difference vanishes only as $h_0 \to \infty$. We have also found that for $h_{0_A} \neq h_{0_B}$ the phase relation between individual precessions is lost and no entanglement preservation is consequently observed.

We now switch off the magnetic field on both qubits (i.e. we take $h_0 = 0$) and apply a finite field $h > 0$ on the environments. In this case, a particularly interesting effect is observed as h becomes larger than the saturation value $h = J$ and the dynamics of both chains slow down. As a consequence, after the transient, the dynamics of the correlations between the two qubits are considerably suppressed, due to the difficulty faced by the qubits to exchange excitations with saturated environments. A long-time entanglement memory effect results from this, which is evident in figure 6(a). There, we also notice a reduction of the wiggling, which further witnesses the freezing of the entanglement dynamics. It should be noted that such an effect is profoundly different from the decoupling mechanism highlighted previously, where $\bar{C}_a - \bar{C}_p$ was a monotonic function of the magnetic field. Here, in fact, a peak occurs in the difference between time-averaged concurrence components when $h = J$, as shown in figure 6(b), revealing a drastic change in the entanglement behavior at the onset of an environmental QPT [20]. Clearly, at the

environmental critical point, the antiparallel entanglement is favored against the parallel one, which is at the origin of the peculiar behavior observed in figure 6(b) for the dashed line. The drastic change in the behavior of the average concurrence observed at $h/J = 1$ is unique for the mechanism discussed here and, as already stressed, clearly distinguished from the freezing effect due to mismatched frequencies at each qubit–environment subsystem. For $h > J$, the effect is fully established and the average concurrence increases, while $\overline{C}_a$ and $\overline{C}_p$ get closer to each other. Moreover, by defining $\mathcal{Z}(t) = (1/2t^2) \sum_{n=1}^{N} (n+1)^2 \mathcal{J}_{n+1}^2(2t)$ and using the exact analytical expressions (valid for $h > J$),

$$
C_a(t) = 2 \max\left\{ 0, \gamma(t) - \sqrt{\frac{1}{16} - \frac{\left[\gamma^2(t) + \mathcal{Z}^2(t)\right]}{2} + \left[\gamma^2(t) - \mathcal{Z}^2(t)\right]^2} \right\},
$$

$$
C_p(t) = 2 \max\left\{ 0, \gamma(t) + \gamma^2(t) + \mathcal{Z}^2(t) - \tfrac{1}{4} \right\},
$$

(24)

we see that when the environments are saturated (i.e. all the spins of the chains are aligned along the z-axis), the concurrence dynamics do not depend on the magnetic field.

4.2. Anisotropic coupling

We finally consider the case of anisotropic coupling $J_0^x \neq J_0^y$ between each qubit and its respective environment (the chain). Differently from the case of isotropic coupling studied in section 4.1, and as a direct consequence of the fact that the total magnetization of A and B is not conserved, the off-diagonal elements $\tilde{\rho}_{23}$ and $\tilde{\rho}_{14}$ of the two-qubit reduced density matrix are not dynamically disjoint. This implies the possibility for the concurrence of the two-qubit state to switch from the parallel to the antiparallel type and vice versa.

For the sake of clarity, we consider extremely anisotropic conditions, setting $J_{0_\kappa}^y = 0$. In the case of no magnetic field on both qubits, $h_0 = 0$, a very simple expression for the concurrence is found, due to the fact that $\langle \hat{s}_{0_\kappa}^x(t) \rangle$ is a constant of motion. In particular, if the two qubits are initially prepared in a combination of the two antiparallel Bell states, their concurrence will evolve as $C_{\uparrow\downarrow}(t) = -C_{\uparrow\uparrow}(t) = \Pi_{0_A}^y(t) \Pi_{0_B}^y(t)$. On the other hand, if parallel Bell states are used to build up the initial entangled state, it is $C_{\uparrow\uparrow}(t) = -C_{\uparrow\downarrow}(t) = \Pi_{0_A}^y(t) \Pi_{0_B}^y(t)$. As a consequence, if $\Pi_{0_A}^y(t) = \Pi_{0_B}^y(t)$ (holding when $\hat{\mathcal{H}}_A = \hat{\mathcal{H}}_B$), the two-qubit concurrence cannot switch between $C_{\uparrow\uparrow}$ and $C_{\uparrow\downarrow}$. On the contrary, if $\Pi_{0_A}^y(t) \neq \Pi_{0_B}^y(t)$, one can drive the two-qubit system from parallel-type to antiparallel and vice versa. In fact, the switching between parallel and antiparallel entanglements is observed when $\hat{s}_{0_A}$ and $\hat{s}_{0_B}$ are flipped, under the effect of the coupling with the first spin of their respective chain, at different frequencies (for instance, when $J_A^x \neq J_B^x$), or when the dynamics of one subsystem are slowed down with respect to the other (for instance, due to the fact that the field on one of the two chains is larger than the saturation value, as seen in section 4.1). However, as discussed in [3], a two-channel entanglement evolution has an upper bound given by the product of the one-channel dynamics. Therefore, for such an 'entanglement switching' to occur, the Hamiltonian parameters of subsystems A and B should be set so as to retain high entanglement values. By fixing J_B^x, while setting $h_A \gg J_A^x$ in order to slow down the entanglement relaxation in the corresponding channel, the efficiency of the switching increases. This is clearly seen in figure 7. On the other hand, we can decrease J_A^x so that channel B is far more responsible for the entanglement evolution. In this case too, a very
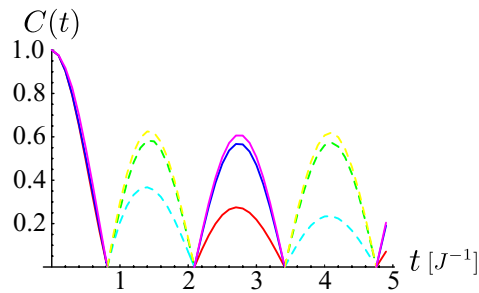
Figure 7. Concurrence between Q_A and Q_B for anisotropic coupling, $J_{0_A}^x = J_{0_B}^x = J$. The magnetic fields are set to zero everywhere but on the chain Γ_A, where the field is allowed to change within the saturation region, $h_A = 1, 2$ and 10 (bottom to top). Solid (dashed) lines are for $C_{\uparrow\uparrow}$ ($C_{\uparrow\downarrow}$). All quantities are dimensionless.

efficient switching mechanism is achieved, suggesting that the saturation region of the chain is associated with an effective decoupling of the qubit from its corresponding environment. Finally, we note that, the coefficients defined by equations (8) being regular oscillating functions of time, the concurrence can only vanish on a countable number of points on the temporal axis and cannot remain null for finite intervals of time. Therefore, entanglement sudden death is not observed.

5. Conclusions

We have analyzed the dynamics of an entangled qubit pair connected to two structured environments composed of open-ended and finite interacting spin chains. The intra-chain interaction has been modeled by an XX Heisenberg-like Hamiltonian, while the coupling between each qubit and its respective environment has been realized via an XY exchange term with the first spin of the chain. Application of uniform magnetic fields has also been considered. We have exactly determined the time-dependent two-qubit density matrix, starting from the information gathered on the single-qubit dynamics.

We have then provided analytical solutions both for the case of finite even N and in the thermodynamic limit, thus getting access to a comprehensive and general analysis of entanglement evolution. Particular emphasis has been given to the relaxation-like dynamics implied by the specific type of coupling considered, which gives rise, under suitable conditions, to a sudden death of the entanglement that we have analyzed. Interestingly, we have unveiled the occurrence of ESD also when starting from initially pure two-qubit states, a peculiarity of our model that does not emerge under 'longitudinal' qubit–environment couplings.

By manipulating the transverse magnetic field on the initially entangled qubits, we have shown the possibility of decoupling their dynamics from those of their respective environments, thereby allowing for a dynamical entanglement protection. On the other hand, when the magnetic fields applied to both chains are larger than the saturation value, the dynamics of the environments slow down and entanglement sudden death is not observed. Interesting features are observed when the environments undergo a quantum phase transition, which in this case happens when the field applied to the chain obtains the saturation value, in particular as far as the behavior of parallel and antiparallel concurrences is concerned.

Our work provides an analytical characterization of the transverse (i.e. energy exchanging) coupling between a simple and yet interesting out-of-equilibrium system (the two qubits) and a nontrivial spin environment (the two chains). As spin models are now understood as effective descriptions of many different physical systems, our results hold the promise to find fertile applications to a variety of cases. As a particularly interesting situation, one can think about the engineering of an effective spin environment by using unidimensional arrays of small-capacitance superconducting Josephson junctions [21], which show a sharp phase transition from Josephson-type behavior to Cooper-pair tunneling Coulomb blockade analogous to that of an *XY* model. This implementation thus constitutes a nearly ideal test for our predictions, since the effective environmental parameters can be modified through the use of gate voltages and external magnetic fluxes. It would be very interesting to investigate the applicability and relevance of a study such as the one performed here to the investigation of the properties of intrinsically open systems in quantum chemistry and biology exposed to finite-sized environments. In this context, it is particularly significant that the mathematical model used to describe the radical pair mechanism [22] bears some analogies with the central-qubit model.

Acknowledgments

References

[1] Nielsen M A and Chuang I L 2000 *Quantum Computation and Quantum Information* (Cambridge: Cambridge University Press)
[2] Benjamin S C and Browne D E (ed) Special issue of *Int. J. Quantum Inf.* **8**(1–2)
[3] Konrad T, de Melo F, Tiersch M, Kasztelan C, Aragão A and Buchleitner A 2008 *Nature Phys.* **4** 99
[4] Yu T and Eberly J H 2009 *Science* **323** 598
[5] Almeida M P, de Melo F, Hor-Meyll M, Salles A, Walborn S P, Souto Riberiro P H and Davidovich L 2007 *Science* **316** 579
　　Laurat J, Choi K S, Deng H, Chou C W and Kimble H J 2007 *Phys. Rev. Lett.* **99** 180504
[6] Lai C-Y, Hung J-T, Mou C-Y and Chen P 2008 *Phys. Rev.* B **77** 205419
　　Nie Jing Wang L-C and Yi X-X 2009 *Commum. Theor. Phys.* **51** 815
　　Yang W and Liu R-B 2008 *Phys. Rev.* B **78** 085315
　　Yuan S, Katsnelson M I and De Raedt H 2008 *Phys. Rev.* B **77** 184301
[7] Yuan Z-G, Zhang P and Li S-S 2007 *Phys. Rev.* A **76** 042118
[8] Sun Z, Wang X and Sun C P 2007 *Phys. Rev.* A **75** 062312
[9] Cormick C and Paz J P 2008 *Phys. Rev.* A **78** 012357
[10] Hill S and Wootters W K 1997 *Phys. Rev. Lett.* **78** 5022
　　Wootters W K 1998 *Phys. Rev. Lett.* **80** 2245
[11] Rossini D, Calarco T, Giovannetti V, Montangero S and Fazio R 2007 *Phys. Rev.* A **75** 032333
　　Rossini D, Facchi P, Fazio R, Florio G, Lidar D A, Pascazio S, Plastina F and Zanardi P 2008 *Phys. Rev.* A **77** 052112
[12] Di Franco C, Paternostro M, Palma G M and Kim M S 2007 *Phys. Rev.* A **76** 042316

[13] Di Franco C, Paternostro M and Kim M S 2008 *Phys. Rev.* A **77** 020303

[14] Di Franco C, Paternostro M and Palma G M 2008 *Int. J. Quantum Inf.* **6** (Supp 1) 659

[15] Bellomo B, Lo Franco R and Compagno G 2007 *Phys. Rev. Lett.* **99** 160502

[16] Fubini A, Roscilde T, Tognetti V, Tusa M and Verrucchi P 2006 *Eur. Phys. J.* D **38** 563

[17] Sachdev S 1999 *Quantum Phase Transitions* (Cambridge: Cambridge University Press)

[18] Son W, Amico L, Plastina F and Vedral V 2009 *Phys. Rev.* A **79** 022302

[19] Breuer H P and Petruccione F 2002 *The Theory of Open Quantum Systems* (Oxford: Oxford University Press)

[20] Amico L, Baroni F, Patane' D, Tognetti V and Verrucchi P 2006 *Phys. Rev.* A **74** 022322

[21] Chow E, Delsing P and Haviland D B 1997 *Phys. Rev. Lett.* **81** 204

[22] Cai J, Guerreschi G G and Briegel H J 2010 *Phys. Rev. Lett.* **104** 220502